Pacific Journal of Mathematics

THE FOX–HATCHER CYCLE AND A VASSILIEV INVARIANT OF ORDER THREE

SAKI KANOU AND KEIICHI SAKAI

Volume 323 No. 2 April 2023

PACIFIC JOURNAL OF MATHEMATICS
Vol. 323, No. 2, 2023
https://doi.org/10.2140/pjm.2023.323.281

THE FOX–HATCHER CYCLE AND A VASSILIEV INVARIANT OF ORDER THREE

SAKI KANOU AND KEIICHI SAKAI

We show that the integration of a 1-cocycle $I(X)$ of the space of long knots in $\mathbb{R}^3$ over the *Fox–Hatcher* 1-*cycles* gives rise to a Vassiliev invariant of order exactly three. This result can be seen as a continuation of the previous work of the Sakai (2011), proving that the integration of $I(X)$ over the *Gramain* 1-*cycles* is the *Casson invariant*, the unique nontrivial Vassiliev invariant of order two (up to scalar multiplications). The result in the present paper is also analogous to part of Mortier's result (2015). Our result differs from, but is motivated by, Mortier's one in that the 1-cocycle $I(X)$ is given by the *configuration space integrals* associated with graphs while Mortier's cocycle is obtained in a combinatorial way.

1. Introduction

Spaces of smooth embeddings of manifolds are receiving a lot of attention in topology, on the ground that various important methods in algebraic and geometric topology are being applied to the spaces. In this paper we study the space of (*framed*) *long knots* in $\mathbb{R}^3$.

Definition 1.1. A *long knot* is an embedding $f\colon \mathbb{R}^1 \hookrightarrow \mathbb{R}^3$ satisfying $f(x) = (x, 0, 0)$ for any $x \in \mathbb{R}^1$ with $|x| \geq 1$. A *framed long knot* is a smooth map $\tilde{f} = (f, w)\colon \mathbb{R}^1 \to \mathbb{R}^3 \times \mathrm{SO}(3)$ such that f is a long knot, the first column of $w(x) \in \mathrm{SO}(3)$ is equal to $f'(x)/|f'(x)|$ and $w(x)$ is the identity matrix for any $x \in \mathbb{R}^1$ with $|x| \geq 1$. The space of all long knots (respectively framed long knots) is denoted by $\mathcal{K}$ (respectively $\widetilde{\mathcal{K}}$).

The recent studies of $\mathcal{K}$ (and its high dimensional analogues) are revealing relations between the topological nature of $\mathcal{K}$ and the *Vassiliev invariants* (see for example [12]) for knots and links. In [17] Sakai has constructed a de Rham 1-cocycle $I(X)$ of $\mathcal{K}$ (see Section 3), by means of the integrations over configuration spaces associated with a *graph cocycle* X (see Figure 6), and has shown that the integration

Sakai is partially supported by JSPS KAKENHI Grant Number 20K03608.
MSC2020: primary 57K16, 58D10; secondary 81Q30.
Keywords: Spaces of embeddings: Configuration space integrals: the Fox–Hatcher cycle: Vassiliev invariants.

of $I(X)$ over the *Gramain cycles* of $\mathcal{K}$ gives rise to the *Casson invariant* v_2, the Vassiliev invariant of order two uniquely characterized by $v_2(\text{trivial knot}) = 0$ and $v_2(\text{trefoil knot}) = 1$. This may be seen as a real valued version of [19, Theorem 2]. After that Mortier has given another 1-cocycle α_3^1 of $\mathcal{K}$ in a combinatorial way and has shown that its evaluations over the Gramain cycles and the *Fox–Hatcher cycles FH* are Vassiliev invariants of orders respectively two and three [14, Theorem 4.1]. In [7; 8; 10] 1-cocycles on $\mathcal{K}$ are also studied in detail from a combinatorial viewpoint.

The main result in the present paper is analogous to the order three part of Mortier's result.

Theorem 1.2. *The integration of $I(X)$ over the Fox–Hatcher cycles gives rise to a Vassiliev invariant of order three for framed long knots. More precisely we have*

$$\int_{p_*FH_{\tilde{f}}} I(X) = 6v_3(f) - \mathrm{lk}(\tilde{f})v_2(f), \tag{1-1}$$

where

- *$p\colon \widetilde{\mathcal{K}} \to \mathcal{K}$ is the first projection and $f = p(\tilde{f})$,*
- *v_2 is the Casson invariant, and v_3 is the Vassiliev invariant of order three characterized by the conditions*

$$v_3(\textit{trivial knot}) = 0, \quad v_3(3_1^+) = 1, \quad v_3(3_1^-) = -1 \tag{1-2}$$

  (3_1^+ and 3_1^- are respectively the right-handed and the left-handed trefoil knots), and

- *$\mathrm{lk}(\tilde{f}) \in \mathbb{Z}$ is the **framing number** of $\tilde{f}$ (see Remark 1.3 below).*

Remark 1.3. The framing number $\mathrm{lk}(\tilde{f})$ is the linking number of $f = p(\tilde{f})$ and f', where f' is the long knot obtained by moving f slightly into the direction of the second column of w. In fact the map $p \times \mathrm{lk}\colon \widetilde{\mathcal{K}} \to \mathcal{K} \times \mathbb{Z}$ is a homotopy equivalence [5, Proposition 9], and the framing number uniquely determines the framing w up to homotopy. Thus we may regard a framed long knot as a pair (f, w) of $f \in \mathcal{K}$ and $w \in \mathbb{Z}$.

The 1-cocycle $I(X)$ is constructed by means of the *configuration space integral associated with graphs*, that was developed in [1; 4; 13] to describe Vassiliev invariants and was generalized in [6] to obtain a cochain map from a graph complex to $\Omega^*_{DR}(\mathcal{K})$ (up to some correction terms, that vanish in the cases of the spaces of long knots in high dimensional spaces). Vassiliev invariants (which are examples of 0-cocycles of $\mathcal{K}$) are obtained from trivalent graphs, while our 1-cocycle $I(X)$ comes from nontrivalent graphs (see Figure 6). It is very interesting, although not strange, that nontrivalent graphs may also have information of Vassiliev invariants.

We note that the right hand side of (1-1) coincides with the formula for Mortier's invariant of order three. We thus expect that the 1-cocycle $I(X)$ is cohomologous to Mortier's α_3^1. This is true on the connected components of torus and hyperbolic knots, since $I(X)$ agrees with α_3^1 on the Gramain and the Fox–Hatcher cycles by Theorem 1.2, [17, Theorem 3.1] and [14, Theorem 4.1], and these cycles generate π_1 of the components of torus and hyperbolic knots [11, page 2].

This paper is organized as follows: In Section 2 the Fox–Hatcher cycle is introduced, and in Section 3 the construction of the 1-cocycle $I(X)$ is reviewed. Our invariant v, the left hand side of (1-1), is shown to be of order three in Corollary 4.2. The key ingredient is Theorem 4.1 and is proved in Section 4B. The formula (1-1) is verified in Section 4C.

2. The Fox–Hatcher cycle

2A. ***The Fox–Hatcher cycle.*** The Fox–Hatcher cycle was introduced in [9], and was later studied in [11] from the viewpoint of the space of knots. If $f = p(\tilde{f})$ is not trivial, it then gives a nonzero element of $\pi_1(\widetilde{\mathcal{K}}_{\tilde{f}})$, where $\widetilde{\mathcal{K}}_{\tilde{f}}$ is the path component of $\widetilde{\mathcal{K}}$ containing $\tilde{f}$.

The Fox–Hatcher cycle is defined as follows. A framed long knot can be seen as a based embedding $f\colon S^1 \hookrightarrow S^3$ (we see S^3 as in $\mathbb{R}^4 \approx \mathbb{C}^2$) together with a framing w, with a prescribed behavior near the basepoint. For $t \in S^1$, $w(t)$ is an orthonormal basis of $T_{f(t)}S^3$ whose first vector is $f'(t)/|f'(t)|$. There exists an S^1-action on the space of such embeddings defined by $(\theta \cdot (f, w))(t) := (A(\theta)^{-1} f(t-\theta), A(\theta)^{-1} w(t-\theta))$, where $A(\theta) \in \mathrm{SO}(4)$ is the matrix given by $A(\theta) = (w(\theta), f(\theta))$. For any $\tilde{f} \in \widetilde{\mathcal{K}}$, this action determines a 1-cycle $FH_{\tilde{f}}\colon S^1 \to \widetilde{\mathcal{K}}_{\tilde{f}}$ and we call it the *Fox–Hatcher cycle*. We notice that the S^1-action looks very similar to the natural S^1-action on free loop spaces by the reparametrization, and in fact this action defines a *BV-operation* on $H_*(\widetilde{\mathcal{K}})$ [18].

Practically it is convenient to describe FH on knot diagrams. In this paper a framed long knot is drawn in a usual knot diagram with so-called *blackboard framing*.

Definition 2.1. Let D be a knot diagram of $\tilde{f}$ with blackboard framing and c the "left-most" crossing, namely the crossing that we meet first when traveling from $f(-1)$ along the natural orientation of f. We call the transformation shown in Figure 1 the *Fox–Hatcher move* (FH-move for short) *on* c.

The left-most crossing c disappears after the FH-move on c and the right-most crossing c' is created. If the arc that moves in the FH-move is the over-arc (resp. under-arc) at c, then after the FH-move it becomes the over-arc (resp. under-arc) at c'. We arrive the original diagram D after performing the FH-moves for all

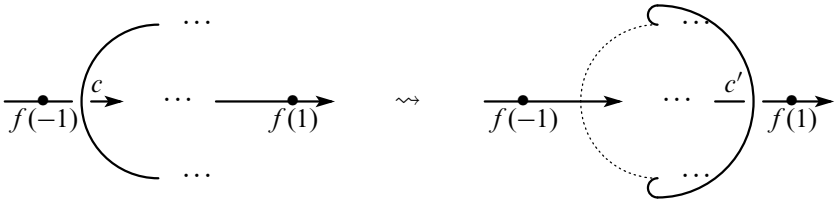

Figure 1. The Fox–Hatcher move on c.

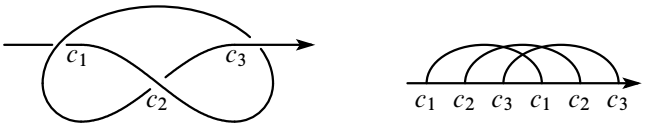

Figure 2. A knot diagram and its Gauss diagram.

the other crossings c of D and the newborn crossings c'. The sequence of these FH-moves realizes $FH_{\tilde{f}}$.

2B. ***FH moves and Gauss diagrams.*** The configuration of crossings of a knot diagram is encoded by (*linear*) *Gauss diagrams*. Here we see how the FH-move on the left-most crossing changes the Gauss diagram.

Definition 2.2. A (*linear*) *Gauss diagram* is a partition of $\{1, 2, \ldots, 2n\}$ for some natural number n into a union $\bigcup_{1\le k\le n}\{i_k, j_k\}$ of n subsets of cardinality 2.

A Gauss diagram can be seen as a graph on $\mathbb{R}^1$ with an even number of vertices all of which are on $\mathbb{R}^1$ and with each vertex joined by exactly one edge with another vertex. Here segments in $\mathbb{R}^1$ interposed between two vertices are not regarded as edges. See Figure 2 for example.

Definition 2.3 [17, Definition 3.3]. Let $c_1, \ldots, c_n$ be (part of the) crossings of a knot diagram of $f \in \mathcal{K}$ such that each c_i corresponds to $f(p_i)$ and $f(q_i)$, with $-1 < p_1 < \cdots < p_n < 1$ and $p_i < q_i$ for any $i = 1, \ldots, n$. We say that the crossings $c_1, \ldots, c_n$ *respect* a Gauss diagram G if G is isomorphic to the Gauss diagram $G_{c_1,\ldots,c_n}$ obtained by joining p_i and q_i for $i = 1, \ldots, n$. See Figure 2.

Under the setting of Definition 2.3, the left-most crossing is c_1. Let G be the Gauss diagram that $c_1, \ldots, c_n$ respect. Then the new knot diagram obtained by performing the FH-move on c_1 has crossings $c_2, \ldots, c_n, c_1'$ that respect the Gauss diagram G' obtained by moving the left-most vertex (corresponding to c_1) to the right-most one. See Figure 3.

We eventually arrive the original Gauss diagram after performing the FH-moves on all the crossings c of the original diagram and the newborn crossings c'. This sequence produces a cycle of Gauss diagrams (see Figures 7, 8, 9). In this way the set of all the Gauss diagrams is decomposed into the disjoint cycles.

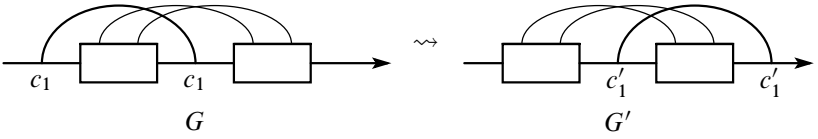

Figure 3. The FH-move on c_1 on the Gauss diagram.

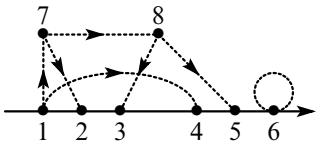

Figure 4. An example of graphs; the i-vertices are those labeled by $1, \dots, 6$ and the f-vertices are those labeled by 7, 8, and there is a loop at the i-vertex labeled by 6.

3. The cocycle $I(X)$

In this section we give a quick review of the construction of differential forms on $\mathcal{K}$ associated with graphs. See also [1; 4; 6; 13; 20] for details.

By a *graph* we mean the oriented real line $\mathbb{R}^1$ together with two kind of vertices, one is called *interval* and the other *free*, and *oriented edges* connecting them (see Figure 4).

The interval vertices (or i-vertices for short) are placed on the oriented line while the free vertices (or f-vertices for short) are not on the line. The i-vertices and the f-vertices of a graph X are labeled by respectively the numbers $1, \dots, \mathrm{v_i}$ and $\mathrm{v_i}+1, \dots, \mathrm{v_i}+\mathrm{v_f}$, where $\mathrm{v_i}$ and $\mathrm{v_f}$ are respectively the numbers of the i-vertices and the f-vertices of X, so that the labels of the i-vertices respect the orientation of the real line. We allow graphs to have loops, where a *loop* is an edge that has exactly one i-vertex as its endpoint (see Figure 4).

For a graph X, let E_X be the configuration space

$$E_X := \big\{(f, (y_1, \dots, y_{\mathrm{v_i}+\mathrm{v_f}})) \in \mathcal{K} \times \mathrm{Conf}_{\mathrm{v_i}+\mathrm{v_f}}(\mathbb{R}^3) \mid y_i = f(x_i) \text{ for some } x_i \in \mathbb{R}^1 \text{ for } i = 1, \dots, \mathrm{v_i}\big\}, \tag{3-1}$$

where

$$\mathrm{Conf}_k(M) := \{(x_1, \dots, x_k) \in M^{\times k} \mid x_i \neq x_j \text{ if } i \neq j\} \tag{3-2}$$

is the space of k-point configurations on a space M.

To an oriented edge α of X from the i-th vertex to the j-th vertex ($i \neq j$), we assign a map

$$\varphi_\alpha \colon E_X \to S^2, \quad \varphi_\alpha(f, (y_1, \dots, y_{v_i+v_f})) := \frac{y_j - y_i}{|y_j - y_i|}. \tag{3-3}$$

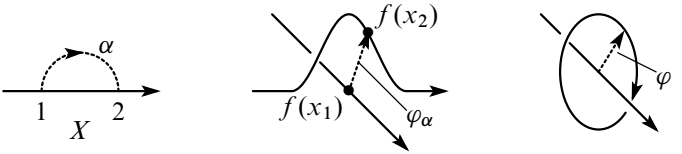

Figure 5. The graph X in Example 3.2 (the left), configurations where the image of φ_α is contained in supp(vol) (the center), the Hopf link (the right).

To a loop α at k-th i-vertex ($1 \le i \le \mathrm{v_i}$) we assign

$$\varphi_\alpha \colon E_X \to S^2, \quad \varphi_\alpha(f, (y_1, \dots, y_{v_i+v_f})) := \frac{f'(x_k)}{|f'(x_k)|}, \tag{3-4}$$

where $x_k \in \mathbb{R}^1$ satisfies $y_k = f(x_k)$.

Let $\mathrm{vol} \in \Omega^2_{DR}(S^2)$ be a unit volume form of S^2 that is antisymmetric, meaning that $i^* \mathrm{vol} = -\mathrm{vol}$ for the antipodal map $i \colon S^2 \to S^2$. Define $\omega_X \in \Omega^{2e}_{DR}(E_X)$ by

$$\omega_X := \bigwedge_{\text{edges } \alpha \text{ of } X} \varphi_\alpha^*(\mathrm{vol}), \tag{3-5}$$

where e is the number of edges of X. The order of the edges is not important because $\deg \mathrm{vol} = 2$ is even.

Let $\pi_X \colon E_X \to \mathcal{K}$ be the first projection. This is a fiber bundle with fiber

$$\pi_X^{-1}(f) = \{y \in \mathrm{Conf}_{\mathrm{v_i}+\mathrm{v_f}}(\mathbb{R}^3) \mid y_i = f(x_i) \text{ for some } x_i \in \mathbb{R}^1 \text{ for } i = 1, \dots, \mathrm{v_i}\} \tag{3-6}$$

of dimension $\mathrm{v_i} + 3\mathrm{v_f}$. Integrating ω_X along the fiber, we get

$$I(X) := \pi_{X*}(\omega_X) \in \Omega^{2e-\mathrm{v_i}-3\mathrm{v_f}}_{DR}(\mathcal{K}). \tag{3-7}$$

Remark 3.1. The integration (3-7) converges since we can compactify all the fibers of π_X by adding the boundary faces to (3-6) so that the maps φ_α are smoothly extended to the compactification. See [3; 4; 6; 13].

Example 3.2. Let X be the graph that has only one edge α joining two i-vertices (Figure 5, the left).

Then $E_X \approx \mathcal{K} \times \mathrm{Conf}_2(\mathbb{R}^1)$ and $I(X) \in \Omega^0_{DR}(\mathcal{K})$ is a function on $\mathcal{K}$, but is not a locally constant function (i.e., not an isotopy invariant), as we see below.

In this paper we use an antisymmetric unit volume form vol whose support is contained in (small) neighborhoods $U_\pm$ of the poles $(0, 0, \pm 1) \in S^2$. Suppose $f \in \mathcal{K}$ is "almost planer," meaning that

- the image of f coincides with a knot diagram D on $\mathbb{R}^2 \times \{0\}$ except for neighborhoods of crossings of D,
- near the crossings the image of f is contained in $\mathbb{R}^2 \times (-\epsilon, \epsilon)$, and
- the unit tangent vectors $f'(x)/|f'(x)|$ are not contained in $U_\pm$.

Then $\varphi_\alpha\colon \{f\}\times \mathrm{Conf}_2(\mathbb{R}^1)\to S^2$ has its image in $U_\pm$ only on the subspace of (x_1,x_2) such that $f(x_1)$ and $f(x_2)$ are on the over- and under-arcs of a crossing of D, one on each arc (Figure 5, the center). Each crossing contributes to the value $I(X)(f)$ by half of its sign; because this contribution is the half of the linking number of the Hopf link (Figure 5, the right), which is equal to the sign of the crossing.

By the generalized Stokes' theorem for fiber integrations, we have

$$dI(X)=\pi_{X*}(d\omega_X)\pm\pi^{\partial}_{X*}(\omega)=\pm\pi^{\partial}_{X*}(\omega), \tag{3-8}$$

where π^{∂}_X is the restriction of π_X to the fiberwise boundary. There exists "almost" 1-1 correspondence between

- the codimension 1 faces of the boundary that nontrivially contribute to $dI(X)$, and
- the graphs obtained from X by contracting one of its edges and *arcs* (segments in $\mathbb{R}^1$ interposed between two i-vertices).

Here we in fact need the antisymmetry of vol. We thus have

$$dI(X)=I(\partial X)+(\text{correction terms}), \tag{3-9}$$

where ∂X is a formal sum of graphs obtained from X by contracting one of its edges and arcs. The above correspondence is not rigorously 1-1 and we need "correction terms," that are conjectured to vanish. We can therefore get a closed form of $\mathcal{K}$ if we have a *graph cocycle*, a formal sum X of graphs with $\partial X=0$ (and if we have appropriate correction terms). It is known that any $\mathbb{R}$-valued Vassiliev invariant can be produced from a *trivalent* graph cocycle.

In [16; 17] Sakai has given an example of *nontrivalent* graph cocycle

$$X=\sum_{1\le k\le 9} a_k X_k,\quad (a_1,\dots,a_9)=(-2,1,2,-2,2,-1,1,-1,1) \tag{3-10}$$

(see Figure 6), and has proved that $I(X)\in H^1_{DR}(\mathcal{K})$ is not zero.[1] This follows from:

Theorem 3.3 [17]. *The differential form $I(X)\in\Omega^1_{DR}(\mathcal{K})$ is closed, and its integration over the* ***Gramain cycle*** *G_f (see Remark 3.4 below) is equal to the* ***Casson invariant*** *$v_2(f)$.*

[1]The coefficients a_7, a_8, a_9 in [16; 17] are wrong and those in (3-10) are correct. The main results in [16; 17] still hold since the graphs X_7, X_8, X_9 are not essential in the integration of $I(X)$ over the Gramain cycles. See [16, Lemma 4.2].

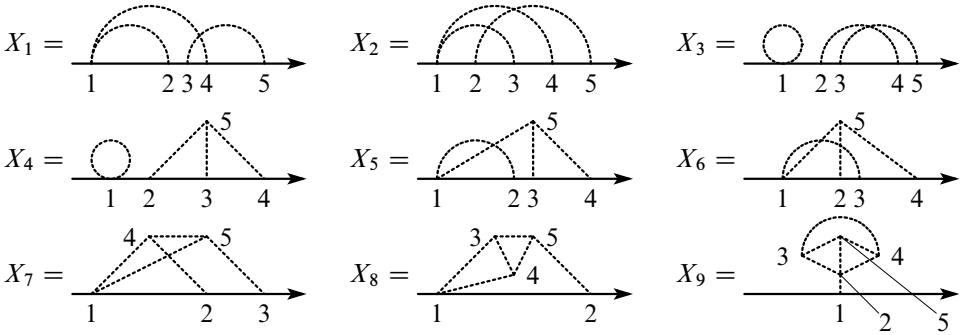

Figure 6. The graphs $X_1, \dots, X_9$ that give a graph cocycle $\sum_i a_i X_i$; the edges are oriented from the vertex with the smaller labels.

Remark 3.4. The *Gramain* 1*-cycle* $G_f\colon S^1 \to \mathcal{K}$ for $f \in \mathcal{K}$ is a cycle that rotates f around the "long axis" $\mathbb{R}^1 \times \{(0,0)\}$. Explicitly G_f is given by

$$G_f(\theta)(x) := \begin{pmatrix} 1 & & \\ & \cos\theta & \\ & & \sin\theta \end{pmatrix} f(x) \quad \text{for } \theta \in S^1, x \in \mathbb{R}^1. \tag{3-11}$$

Mortier [14, Theorem 4.1] has given a 1-cocycle α_3^1 of $\mathcal{K}$ in a combinatorial way and has proved that

$$\langle \alpha_3^1, G_f \rangle = v_2(f) \quad \text{and} \quad \langle \alpha_3^1, p_* FH_{(f,w)} \rangle = 6v_3(f) - w \cdot v_2(f) \tag{3-12}$$

for $(f, w) \in \mathcal{K} \times \mathbb{Z} \simeq \widetilde{\mathcal{K}}$. This result motivates us to compute the integration of $I(X)$ over the FH-cycles. We will give another proof of $\langle I(X), G_f \rangle = v_2(f)$; see Corollary 4.9 (actually this corrects the proof of [17, Theorem 3.1], see Remark 4.11).

4. Integration of $I(X)$ over the Fox–Hatcher cycle

Recall that $p\colon \widetilde{\mathcal{K}} \to \mathcal{K}$ is the map forgetting the framing of $\tilde{f}$. For any $\tilde{f} \in \widetilde{\mathcal{K}}$ we define

$$v(\tilde{f}) := \int_{p_* FH_{\tilde{f}}} I(X) = \sum_{1 \le k \le 9} a_k \int_{p_* FH_{\tilde{f}}} I(X_k). \tag{4-1}$$

This gives an isotopy invariant v for framed long knots. Our goal is to describe v as a linear combination of the Vassiliev invariants of order less or equal to three.

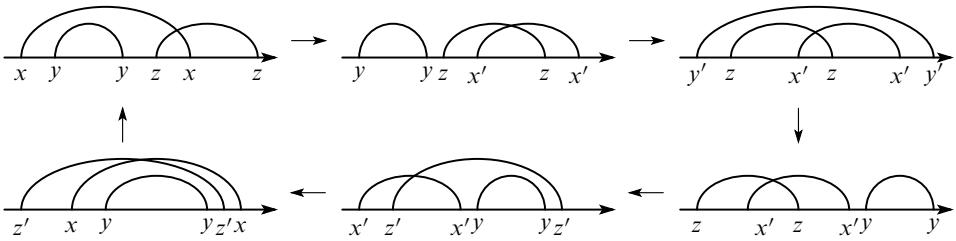

Figure 7. Type I cycle of the Gauss diagrams respecting three crossings under consideration; $\{x, y, z\} = \{c_1, c_2, c_3\}$.

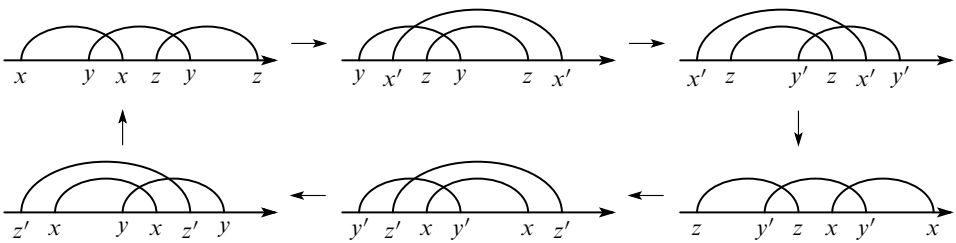

Figure 8. Type II cycle of the Gauss diagrams respecting three crossings under consideration; $\{x, y, z\} = \{c_1, c_2, c_3\}$.

4A. ***The invariant v is of order three.*** For any $\tilde{f} \in \widetilde{\mathcal{K}}$ and crossings $c_1, \ldots, c_n$ of its diagram, define

$$D^n v(\tilde{f}) := \sum_{\epsilon_1,\ldots,\epsilon_n \in \{+1,-1\}} \epsilon_1 \cdots \epsilon_n v(\tilde{f}_{\epsilon_1,\ldots,\epsilon_n}), \tag{4-2}$$

where $\tilde{f}_{\epsilon_1,\ldots,\epsilon_n}$ is a framed long knot obtained by changing, if necessary, the crossings c_i so that its sign is equal to ϵ_i. It should be noticed that $D^n v$ depends on the choice of crossings $c_1, \ldots, c_n$, although it is not explicit in the notation. What we want to show is $D^4 v(\tilde{f}) = 0$ for any choice of $\tilde{f}$ and $c_1, \ldots, c_4$.

Let c_1, c_2, c_3 be (part of the) crossings of a diagram D of $\tilde{f} \in \widetilde{\mathcal{K}}$ respecting the Gauss diagram G (Definition 2.3). Let us perform the FH-moves (described in Section 2) on all the crossings c of D and the corresponding newborn crossings c'. The Gauss diagram that the three crossings under consideration respect changes as in Figure 3 when the FH-move is performed on one of c_i and c_i' $(i = 1, 2, 3)$, and in the sequence of the FH-moves realizing the FH-cycle, six Gauss diagrams (some of which may be equal to each other) respected by the three crossings under consideration form a cycle. Figures 7, 8 and 9 show three such cycles.

There are 15 Gauss diagrams with three edges, and only 10 of them are included in these three cycles. The remaining five Gauss diagrams form the other two cycles, that we omit since in fact they do not contribute to our computation in Section 4B.

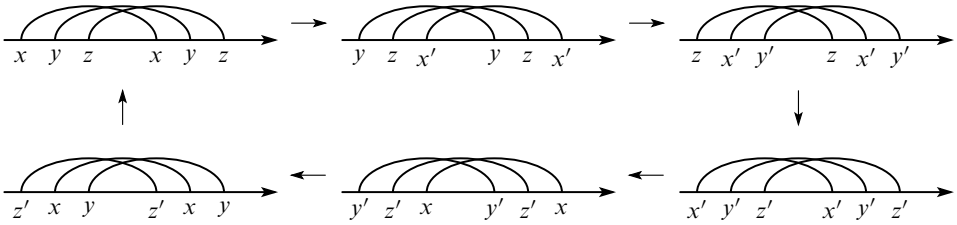

Figure 9. Type III cycle of the Gauss diagrams respecting three crossings under consideration; $\{x, y, z\} = \{c_1, c_2, c_3\}$.

Theorem 4.1. *For any crossings c_1, c_2, c_3, $D^3v(\tilde{f})$ is given by*

(4-3) $D^3v(\tilde{f}) =$

$$\begin{cases} -2 & \text{if } c_1, c_2 \text{ and } c_3 \text{ respect one of the Gauss diagrams in type I cycle,} \\ 2 & \text{if } c_1, c_2 \text{ and } c_3 \text{ respect one of the Gauss diagrams in type II cycle,} \\ 6 & \text{if } c_1, c_2 \text{ and } c_3 \text{ respect the unique Gauss diagram in type III cycle,} \\ 0 & \text{otherwise.} \end{cases}$$

Corollary 4.2. *The invariant v is a Vassiliev invariant for framed long knots of order exactly three.*

Proof. Let $c_1, \ldots, c_4$ be crossings of a diagram of $\tilde{f} \in \widetilde{\mathcal{K}}$. Let $\tilde{f}_\pm$ be knots obtained by changing c_4 so that its sign is respectively ± 1. Then by definition

$$D^4v(f) = D^3v(f_+) - D^3v(f_-). \tag{4-4}$$

Moreover c_1, c_2 and c_3 of f_+ and f_- respect the same Gauss diagram. Thus we have $D^3v(\tilde{f}_+) = D^3v(\tilde{f}_-)$ by Theorem 4.1, concluding $D^4v(\tilde{f}) = 0$.

Theorem 4.1 also says that $D^3v(\tilde{f})$ can be nonzero, and v is not of order two or less. □

The next subsection is devoted to the proof of Theorem 4.1.

4B. ***Computation of D^3v.*** We again remind that D^3v depends on the choice of crossings c_1, c_2, c_3. As in Example 3.2, we assume that

- $\mathrm{vol} \in \Omega^2_{DR}(S^2)$ is an antisymmetric unit volume form of S^2 whose support is contained in small neighborhoods of poles $(0, 0, \pm 1) \in S^2$, and
- we compute $D^3v(\tilde{f})$ after transforming $\tilde{f}$ to be "almost planar."

We moreover assume, just for simplicity, that

- $\tilde{f}$ runs parallel to the x- and y-axes at each crossings (see Figure 15).

For $k = 1, \ldots, 9$, consider the pullback square:

$$\begin{array}{ccccc} (p \circ FH_{\tilde{f}})^* E_{X_k} & & \xrightarrow{\overline{p \circ FH_{\tilde{f}}}} & & E_{X_k} \\ \downarrow{\scriptstyle \pi'_{X_k}} & & & & \downarrow{\scriptstyle \pi_{X_k}} \\ S^1 & \xrightarrow{FH_{\tilde{f}}} & \widetilde{\mathcal{K}} & \xrightarrow{p} & \mathcal{K} \end{array} \tag{4-5}$$

Then

$$\begin{aligned} \int_{p_* FH_{\tilde{f}}} I(X_k) &= \int_{S^1} (p \circ FH_{\tilde{f}})^* \pi_{X_k *} \omega_{X_k} \\ &= \int_{S^1} \pi'_{X_k *} \overline{p \circ FH_{\tilde{f}}}^* \omega_{X_k} \\ &= \int_{(p \circ FH_{\tilde{f}})^* E_{X_k}} \overline{p \circ FH_{\tilde{f}}}^* \omega_{X_k}. \end{aligned} \tag{4-6}$$

Note that $(p \circ FH_{\tilde{f}})^* E_{X_k}$ is explicitly given by

$$\begin{aligned} &(p \circ FH_{\tilde{f}})^* E_{X_k} \\ &\quad = \left\{ (p(FH_{\tilde{f}}(\theta)), y) \in \mathcal{K} \times \mathrm{Conf}_{\mathrm{v_i}+\mathrm{v_f}}(\mathbb{R}^3) \;\middle|\; \begin{array}{l} \theta \in S^1,\ y_i = p(FH_{\tilde{f}}(\theta))(x_i) \\ \text{for some } x_i \in \mathbb{R}^1,\ 1 \le i \le \mathrm{v_i} \end{array} \right\} \\ &\quad \subset E_{X_k}. \end{aligned} \tag{4-7}$$

Suppose a diagram D of $\tilde{f}$ has n crossings. Then $FH_{\tilde{f}}$ can be realized on knot diagram by the sequence of $2n$ FH-moves on c or c', where c is one of the crossings of D and c' is a newly created crossing after the FH-move on c. We can decompose S^1 into $2n$ intervals

$$S^1 = \bigcup_c (I_c \cup I_{c'}) \tag{4-8}$$

such that $FH_{\tilde{f}}$ restricted on I_c (resp. $I_{c'}$) realizes the FH-move on c (resp. c').

Definition 4.3. Under the above setting, define

$$E_{k;c,c'} := \{ (p_*(FH_{\tilde{f}}(\theta)), y) \in (p \circ H_{\tilde{f}})^* E_{X_k} \mid \theta \in I_c \cup I_{c'} \}. \tag{4-9}$$

By definition we have

$$(p \circ FH_{\tilde{f}})^* E_{X_k} = \bigcup_c E_{k;c,c'} \tag{4-10}$$

and hence

$$\int_{(p \circ FH_{\tilde{f}})^* E_X} \omega_{X_k} = \sum_c \int_{E_{k;c,c'}} \overline{p \circ FH_{\tilde{f}}}^* \omega_{X_k}. \tag{4-11}$$

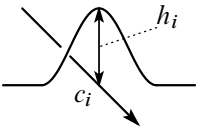

Figure 10. h_i $(i = 1, 2, 3)$.

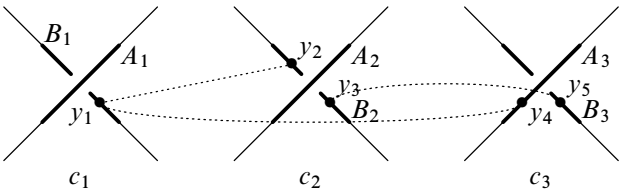

Figure 11. An element of $E_{1;c_1,c_1',A_1}$.

Combining (4-1), (4-2), (4-6) and (4-11), we have

$$D^3v(\tilde{f}) = \sum_{1\le k\le 9} a_k \sum_{c} \sum_{\epsilon_1,\epsilon_2,\epsilon_3\in\{+1,-1\}} \epsilon_1\epsilon_2\epsilon_3 \int_{E_{k;c,c'}} \overline{p\circ FH_{\tilde{f}_{\epsilon_1,\epsilon_2,\epsilon_3}}}^{*}\omega_{X_k}. \tag{4-12}$$

4B1. *Eliminating* $X_3, \ldots, X_9$. Let h_i $(i = 1, 2, 3)$ be the distance between two arcs at c_i, $i = 1, 2, 3$ (Figure 10).

We may compute $D^3v(\tilde{f})$ in the limit $h_i \to 0$ $(i = 1, 2, 3)$ since v is an invariant. In this limit, only the graphs X_1 and X_2 essentially contribute to $D^3v(\tilde{f})$;

Proposition 4.4. (1) *For* $k = 1, \ldots, 9$ *and any crossing* c *other than* c_1, c_2, c_3, *we have*

$$\lim_{h_1,h_2,h_3\to 0} \sum_{\epsilon_1,\epsilon_2,\epsilon_3\in\{+1,-1\}} \epsilon_1\epsilon_2\epsilon_3 \int_{E_{k;c,c'}} \overline{p\circ FH_{\tilde{f}_{\epsilon_1,\epsilon_2,\epsilon_3}}}^{*}\omega_{X_k} = 0. \tag{4-13}$$

(2) *If* $k = 3, \ldots, 9$, *then* (4-13) *also holds for* $c \in \{c_1, c_2, c_3\}$.

Consequently

$$D^3v(\tilde{f}) = \lim_{h_1,h_2,h_3\to 0} \sum_{k=1,2} a_k \times \sum_{c\in\{c_1,c_2,c_3\}} \sum_{\epsilon_1,\epsilon_2,\epsilon_3\in\{+1,-1\}} \epsilon_1\epsilon_2\epsilon_3 \int_{E_{k;c,c'}} \overline{p\circ FH_{\tilde{f}_{\epsilon_1,\epsilon_2,\epsilon_3}}}^{*}\omega_{X_k}. \tag{4-14}$$

Proof of Proposition 4.4 (1). Let $-1 < p_i < q_i < 1$ $(i = 1, 2, 3)$ with $p_1 < p_2 < p_3$ be the real numbers such that $f(p_i)$ and $f(q_i)$ correspond to c_i, and let A_i, B_i be small open intervals that include respectively p_i and q_i (see Figure 11). Let $E_{k;c,c',A_1} \subset E_{k;c,c'}$ be the subspace consisting of (θ, y) with no y_j $(1 \le j \le \mathrm{v_i})$ being in A_1.

Then even if we set $h_1 = 0$, any two points y_j and $y_{j'}$ corresponding to endpoints of a single edge of X_k do not collide in $E_{k;c,c',A_1}$, and the maps φ_α and hence the integrand ω_{X_k} can be defined on $E_{k;c,c',A_1}$. This implies

$$\lim_{h_1\to 0}\left(\int_{E_{k;c,c',A_1}} \overline{p\circ FH_{\tilde{f}_{+1,\epsilon_2,\epsilon_3}}}^{*}\omega_{X_k} - \int_{E_{k;c,c',A_1}} \overline{p\circ FH_{\tilde{f}_{-1,\epsilon_2,\epsilon_3}}}^{*}\omega_{X_k}\right) = 0. \tag{4-15}$$

If we analogously define $E_{k;c,c',A_m}$ and $E_{k;c,c',B_m}$, then similar cancellation to (4-15) occurs for them. Moreover we have

$$\bigcup_{m=1,2,3} (E_{k;c,c',A_m} \cup E_{k;c,c',B_m}) = E_{k;c,c'} \tag{4-16}$$

because no X_k has six or more i-vertices. Although $A_1, \dots, B_3$ are not disjoint, we can arrange them to be disjoint by considering their difference sets and intersections (on which the same argument is valid). Thus we have (4-13). □

Proof of Proposition 4.4 (2) for $k = 7, 8, 9$. It is enough to consider the case $c = c_1$; the cases $c = c_2, c_3$ can be proved similarly.

The similar argument in the proof of (1) also implies (4-15) with A_1 and h_1 replaced respectively by A_m (or B_m) and h_m, $m = 2, 3$. We thus complete the proof, because X_k ($k = 7, 8, 9$) has three or less i-vertices and we have

$$E_{k;c_1,c_1'} = \bigcup_{m=2,3} (E_{k;c_1,c_1',A_m} \cup E_{k;c_1,c_1',B_m}). \tag{4-17}$$ □

Proof of Proposition 4.4 (2) for $k = 5, 6$. It is enough to consider the case $c = c_1$.

Let $E \subset E_{k;c_1,c_1'}$ be the subspace of $E_{k;c_1,c_1'}$ consisting of (θ, y) with each of A_2, B_2, A_3 and B_3 containing at least one y_j corresponding to an i-vertex j of X_k. Then the integrations in (4-13) with $E_{k;c_1,c_1'}$ replaced by $E_{k;c_1,c_1'} \setminus E$ are defined even if we set $h_m = 0$ for at least one $m \in \{2, 3\}$, and the cancellation similar to (4-15) occurs, similarly as the above proof of (2) for $k = 7, 8, 9$. Thus it suffices to show (4-13) with $E_{k;c_1,c_1'}$ replaced by E. Since X_k ($k = 5, 6$) has four i-vertices, each of A_2, B_2, A_3 and B_3 contains exactly one point on E. We divide E into two subspaces:

Type I: The subspace E_I of E consisting of (θ, y) with $y_5 \in \mathbb{R}^3$ outside neighborhoods of c_2 and c_3. Then two i-vertices (4 and 5 in the case of Figure 12) corresponding to the points in $A_m \cup B_m$ are not joined by any edge, for at least one $m = 2, 3$.

Even if we set $h_m = 0$ and these two points may collide, all the maps φ_α and hence ω_{X_k} are still defined on E_I, and the cancellation similar to (4-15) occurs.

Type II: the subspace E_{II} of E consisting of (θ, y) with $y_5 \in \mathbb{R}^3$ in a neighborhood of c_m, $m \in \{2, 3\}$ (see Figure 13; setting $h_2 = 0$ or $h_3 = 0$ are problematic on this subspace).

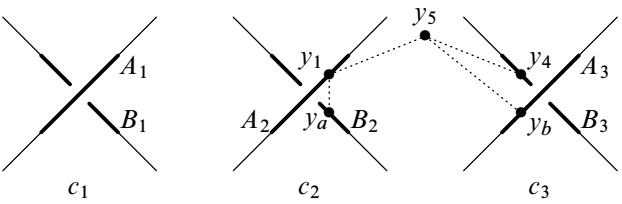

Figure 12. Proposition 4.4(2) for $k = 5, 6$, Type I subspace ($m = 3$, $\{a, b\} = \{2, 3\}$); one of the arcs A_1 and B_1 moves in the FH-move on c_1.

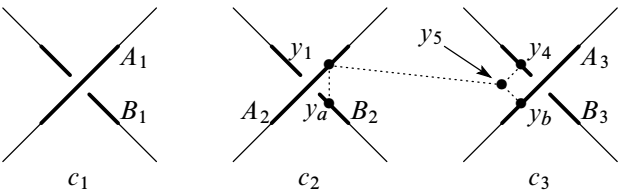

Figure 13. Proposition 4.4(2) for $k = 5, 6$, Type II subspace ($m = 3$, $\{a, b\} = \{2, 3\}$).

On E_{II} at least one edge α of X_k joins the vertex 5 and j with the corresponding point y_j not on $A_m \cup B_m$ ($j = 1$ in the case of Figure 13). Then the image of φ_α is not included in supp(vol) and hence $\varphi_\alpha^* \mathrm{vol} = 0$, because supp(vol) is assumed to be in neighborhoods of $(0, 0, \pm 1) \in S^2$ and our $\tilde{f}$ is almost planar. The integrand ω_{X_k} is therefore zero on E_{II}. □

Proof of Proposition 4.4 (2) for $k = 4$. Consider the case $c = c_1$ (the same arguments are valid for $c = c_2, c_3$). Let $E \subset E_{4;c_1,c_1'}$ be the subspace consisting of (θ, y) where each of A_2, B_2, A_3 and B_3 contains at least one point. It is then enough to show (4-13) with $E_{4;c_1,c_1'}$ replaced by E, as in the above proofs.

As X_4 has four i-vertices, each of A_2, B_2, A_3 and B_3 contains exactly one point on E. In particular $y_1 \in A_2$, and the map φ_α for the loop α at the vertex 1 has the image outside supp(vol) by our assumption on $\tilde{f}$ and vol, and hence ω_{X_4} vanishes on E. □

Proof of Proposition 4.4 (2) for $k = 3$. Again consider the case $c = c_1$. Let $E \subset E_{3;c_1,c_1'}$ be the subspace consisting of (θ, y) satisfying both (i) and (ii):

(i) y_1 is on the arc C that moves in the FH-moves on c_1.

(ii) Each of A_2, B_2, A_3 and B_3 contains exactly one of $y_2, \ldots, y_5$.

Then it suffices to show (4-13) with $E_{3;c_1,c_1'}$ replaced by E. This is because:

- If E' denotes the subspace of $E_{3;c_1,c_1'}$ consisting of (θ, y) that does not satisfy (ii), then the integrations in (4-13) with $E_{3;c_1,c_1'}$ replaced by E' are defined

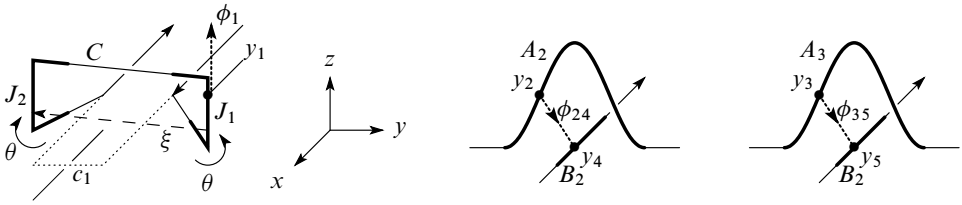

Figure 14. The configuration that can nontrivially contribute to $I(X_3)$.

even if we set $h_m = 0$ for at least one $m \in \{2, 3\}$ and the cancellation similar to (4-15) occurs, by the same reason as in the above proofs.

- If E'' denotes the subspace of $E_{3;c_1,c_1'}$ consisting of (θ, y) that satisfies (ii) but does not satisfy (i). then the map φ_α (α is the loop of X_3 at the i-vertex labeled by 1) has its image outside on supp(vol) since $\tilde{f}$ is supposed to be almost planar, and hence ω_{X_3} vanishes on E''.

Figure 14 shows the configurations in E that may nontrivially contribute to the integration of $I(X_3)$.

Let J_s ($s = 1, 2$) be the unit intervals identified with those on C drawn with thick curves in Figure 14. We write $p_* FH_{\tilde{f}}(\theta)$ as f_θ for short. Define $\phi_1 \colon I_{c_1} \times J_s \to S^2$ ($s = 1, 2$), $\phi_{24} \colon A_2 \times B_2 \to S^2$ and $\phi_{35} \colon A_3 \times B_3 \to S^2$ by

$$\phi_1(\theta, t) := \frac{f_\theta'(t)}{|f_\theta'(t)|}, \quad \phi_{ij}(t, u) := \frac{f(u) - f(t)}{|f(u) - f(t)|}, \quad (i, j) = (2, 4), (3, 5). \tag{4-18}$$

Then

$$\int_E \overline{p \circ FH_{\tilde{f}}}^* \omega_{X_3} = \int_{I_{c_1} \times (J_1 \sqcup J_2)} \phi_1^* \operatorname{vol} \int_{A_2 \times B_2} \phi_{24}^* \operatorname{vol} \int_{A_3 \times B_3} \phi_{35}^* \operatorname{vol}. \tag{4-19}$$

Define the diffeomorphisms $\xi \colon J_1 \to J_2$ and $\eta \colon \mathbb{R}^3 \to \mathbb{R}^3$ by

$$\xi(t) = 1 - t, \quad \eta(x, y, z) := (-x, y, -z). \tag{4-20}$$

Then, with respect to the coordinates of $\mathbb{R}^3$ shown in Figure 14, the following diagram commutes:

$$\begin{array}{ccc} I_{c_1} \times J_1 & \xrightarrow{\phi_1} & S^2 \\ {\scriptstyle \mathrm{id} \times \xi} \downarrow & \circlearrowleft & \downarrow {\scriptstyle \eta} \\ I_{c_1} \times J_2 & \xrightarrow{\phi_1} & S^2 \end{array} \tag{4-21}$$

and since ξ reverses the orientation and η preserves the orientation, we have

$$\int_{I_{c_1} \times J_2} \phi_1^* \operatorname{vol} = - \int_{J_{c_1} \times J_1} \phi_1^* \operatorname{vol} \tag{4-22}$$

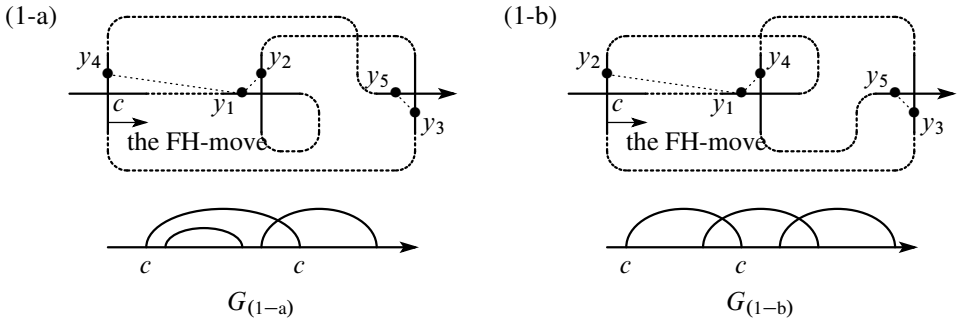

Figure 15. Configurations essentially contributing to $I(X_1)$; they can exist only if the three crossings under consideration respect the Gauss diagrams $G_{(1\text{-a})}$ or $G_{(1\text{-b})}$.

and hence

$$\int_{I_{c_1}\times(J_1\sqcup J_2)} \phi_1^* \,\mathrm{vol} = \sum_{s=1,2} \int_{I_{c_1}\times J_s} \phi_1^* \,\mathrm{vol} = 0. \tag{4-23}$$

Thus (4-19) is zero. □

Thus we only need to compute the alternating sums of the integrations of $I(X_1)$ and $I(X_2)$ in the limit $h_1, h_2, h_3 \to 0$.

4B2. *Computation of* $I(X_1)$. The following two subspaces of $E_{1;c_j,c'_j}$ $(j = 1, 2, 3)$ do not essentially contribute to the alternating sum of $I(X_1)$.

- The subspace where the arc near the left-most crossing moving in the FH-move contains no point; because the integrals on the subspace are the same for $\epsilon_j = +1$ and $\epsilon_j = -1$ and they cancel in the alternating sum.
- The subspace where no edge joins points on A_m and B_m $(m = 2, 3)$; because all the maps φ_α and hence the integrand ω_{X_1} can be defined even if $h_m = 0$ and thus the cancellation similar to (4-15) occurs.

Thus only the subspaces of types (1-a) and (1-b) consisting of (θ, y) as shown in Figure 15 can essentially contribute to the integrations of $I(X_1)$.

In both cases, the arc near the left-most crossing containing y_2 (case (1-a)) or y_4 (case (1-b)) moves to right in the FH-move, and when the arc comes over or under the middle crossing, the map φ_{12} or φ_{14} has its image in supp(vol) and the integrand is not zero at that moment.

If three crossings c_1, c_2, c_3 under consideration respect one of the Gauss diagrams in the Type I cycle (Figure 7), then in the FH-cycle we meet the situation (1-a) in Figure 15 once, because the Gauss diagram $G_{(1\text{-a})}$ appears once in the Type I cycle. If c_1, c_2, c_3 respect one of the Gauss diagrams in the Type II cycle (Figure 8), then in the FH-cycle we meet the situation (1-b) in Figure 15 twice, because the Gauss

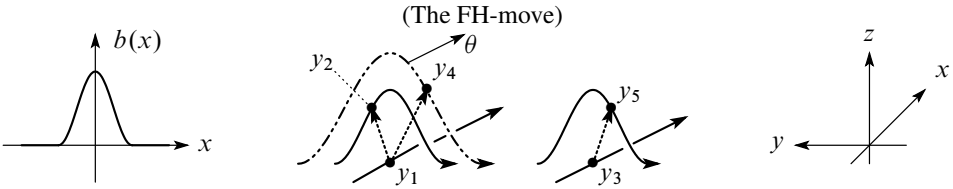

Figure 16. Proof of Proposition 4.5; the case (1-a).

diagram $G_{(1\text{-b})}$ appears twice in the Type II cycle. Otherwise we do not meet the situations (1-a) nor (1-b) and the integration vanishes.

Proposition 4.5. *We have*

$$\epsilon_1\epsilon_2\epsilon_3 \sum_{c\in\{c_1,c_2,c_3\}} \int_{E_{1;c,c'}} \overline{p\circ FH_{\tilde{f}_{\epsilon_1,\epsilon_2,\epsilon_3}}}^{*}\omega_{X_1} \tag{4-24}$$
$$= \begin{cases} \frac{1}{8} & \text{if } c_1, c_2, c_3 \text{ respect one of the Gauss diagrams in Type I cycle,} \\ -\frac{1}{4} & \text{if } c_1, c_2, c_3 \text{ respect one of the Gauss diagrams in Type II cycle,} \\ 0 & \text{otherwise;} \end{cases}$$

see Figures 7 and 8 for Type I and II cycles, respectively.

Proof. Consider the first case; we may assume that c_1, c_2, c_3 respect the Gauss diagram $G_{(1\text{-a})}$. Then only $E_{1;c_1,c_1'}$ can contain the configurations of type (1-a) and nontrivially contribute to the alternating sum of the integrations of $I(X_1)$.

Let $b\colon \mathbb{R}^1 \to \mathbb{R}^1$ be a smooth even function whose graph looks as in Figure 16. For $(\theta, x_1, \dots, x_5) \in \mathbb{R}^6$, consider $y_1, \dots, y_5 \in \mathbb{R}^3$ given by

$$\begin{aligned} y_1 &= (x_1, 0, 0), \\ y_2 &= (0, -\epsilon_2 x_2, b(\epsilon_2 x_2)), \\ y_3 &= (x_3, 0, 0), \\ y_4 &= (\theta, -\epsilon_1 x_4, 2b(\epsilon_1 x_4/2)), \\ y_5 &= (0, -\epsilon_3 x_5, b(\epsilon_3 x_5)) \end{aligned} \tag{4-25}$$

and define $\varphi\colon \mathbb{R}^6 \to (S^2)^{\times 3}$ by

$$\varphi(\theta, x_1, \dots, x_5) := \left(\frac{y_2 - y_1}{|y_2 - y_1|}, \frac{y_5 - y_3}{|y_5 - y_3|}, \frac{y_4 - y_1}{|y_4 - y_1|} \right). \tag{4-26}$$

Then changing the variables suitably, the left hand side of (4-24) is equal to

$$\epsilon_1\epsilon_2\epsilon_3 \int_{\mathbb{R}^6} \varphi^*(\mathrm{vol}^{\times 3}), \tag{4-27}$$

where $\mathrm{vol}^{\times 3} = \mathrm{pr}_1^* \mathrm{vol} \wedge \mathrm{pr}_2^* \mathrm{vol} \wedge \mathrm{pr}_3^* \mathrm{vol} \in \Omega^6_{DR}((S^2)^{\times 3})$.

Define $\Phi\colon \mathbb{R}^6 \to (\mathbb{R}^2)^{\times 3}$ and $\psi_s\colon \mathbb{R}^2 \to S^2$ $(s = 1, 2)$ by respectively

$$\Phi(\theta, x_1, \dots, x_5) := ((x_1, \epsilon_2 x_2), (x_1 - \theta, \epsilon_1 x_4), (x_3, \epsilon_3 x_5)), \tag{4-28}$$

$$\psi_1(x, x') := \frac{y' - y}{|y' - y|}, \quad \psi_2(x, x') := \frac{y'' - y}{|y'' - y|}, \tag{4-29}$$

where $y := (x, 0, 0)$, $y' := (0, -x', b(x'))$, $y'' = (0, -x', 2b(x'/2))$. Then Φ is a linear diffeomorphism whose determinant is $\epsilon_1\epsilon_2\epsilon_3$, and the following diagram is commutative:

(4-30)

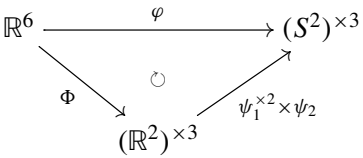

Thus (4-27) is equal to

$$(\epsilon_1\epsilon_2\epsilon_3)^2 \left(\int_{\mathbb{R}^2} \psi_1^* \operatorname{vol} \right)^2 \int_{\mathbb{R}^2} \psi_2^* \operatorname{vol} = \left(\tfrac{1}{2}\right)^3 = \tfrac{1}{8}, \tag{4-31}$$

here $\frac{1}{2}$ appears by exactly the same reason as in Example 3.2.

The second case that c_1, c_2, c_3 respect the Gauss diagram $G_{(1\text{-b})}$ can be similarly computed, replacing

- (4-25) and (4-26) respectively with

$$\begin{aligned} y_1 &= (x_1, 0, 0), \\ y_2 &= (\theta, -\epsilon_2 x_2, b(\epsilon_2 x_2/2)), \\ y_3 &= (x_3, 0, 0), \\ y_4 &= (0, -\epsilon_1 x_4, b(\epsilon_1 x_4)), \\ y_5 &= (0, -\epsilon_3 x_5, b(\epsilon_3 x_5)), \end{aligned} \tag{4-32}$$

$$\varphi(\theta, x_1, \dots, x_5) := \left(\frac{y_4 - y_1}{|y_4 - y_1|}, \frac{y_5 - y_3}{|y_5 - y_3|}, \frac{y_2 - y_1}{|y_2 - y_1|} \right) \tag{4-33}$$

  (namely y_2 and y_4 are swapped), and

- (4-28) with

$$\Phi(\theta, x_1, \dots, x_5) := ((x_1, \epsilon_2 x_2), (x_1 - \theta, \epsilon_1 x_4), (x_3, \epsilon_3 x_5)). \tag{4-34}$$

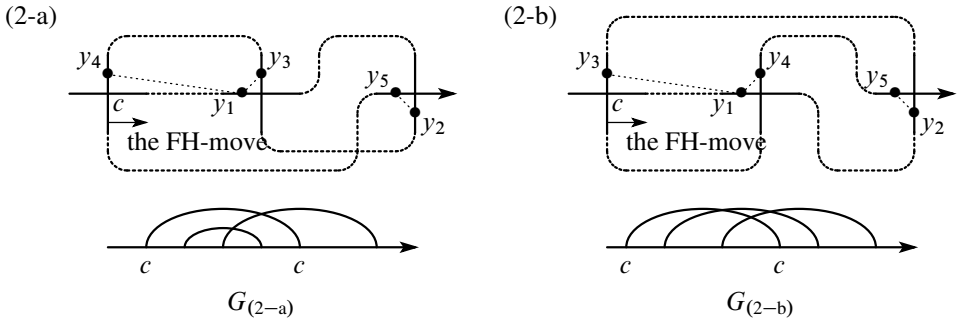

Figure 17. Configurations essentially contributing to $I(X_2)$; they can exist only if the three crossings under consideration respect the Gauss diagrams $G_{(2\text{-a})}$ or $G_{(2\text{-b})}$.

Then the determinant of Φ is $-\epsilon_1\epsilon_2\epsilon_3$, and because we meet the situation (1-b) twice in the FH-cycle, the left-hand side of (4-24) in this case is equal to

$$-2(\epsilon_1\epsilon_2\epsilon_3)^2\left(\int_{\mathbb{R}^2}\psi_1^*\,\mathrm{vol}\right)^2\int_{\mathbb{R}^2}\psi_2^*\,\mathrm{vol}=-\tfrac{1}{4}. \tag{4-35}$$

□

4B3. *Computation of $I(X_2)$.* The computation of $I(X_2)$ goes similarly to that of $I(X_1)$. Only the subspaces of types (2-a) and (2-b) consisting of (θ, y) as shown in Figure 17 can essentially contribute to the alternating sum of the integrations of $I(X_2)$.

If three crossings c_1, c_2, c_3 under consideration respect one of the Gauss diagrams in Type II cycle (Figure 8), then in the FH-cycle we meet the situation (2-a) in Figure 15 twice, because the Gauss diagram $G_{(2\text{-a})}$ appears twice in Type II cycle. If c_1, c_2, c_3 respect one of the Gauss diagrams in Type III cycle (Figure 9), then in the FH-cycle we meet the situation (2-b) in Figure 15 six times, because the Gauss diagram $G_{(2\text{-b})}$ appears six times in Type III cycle.

Proposition 4.6. *We have*

$$\epsilon_1\epsilon_2\epsilon_3\sum_{c\in\{c_1,c_2,c_3\}}\int_{E_{2;c,c'}}\overline{p\circ FH_{\tilde{f}_{\epsilon_1,\epsilon_2,\epsilon_3}}}^{\,*}\omega_{X_2} \tag{4-36}$$
$$=\begin{cases}-\frac{1}{4} & \text{if } c_1,c_2,c_3 \text{ respect one of the Gauss diagrams in Type II cycle,}\\ \frac{3}{4} & \text{if } c_1,c_2,c_3 \text{ respect one of the Gauss diagrams in Type III cycle,}\\ 0 & \text{otherwise;}\end{cases}$$

see Figures 8 and 9 for Type II and III cycles, respectively.

Proof. Consider the first case that c_1, c_2, c_3 respect the Gauss diagram $G_{(2\text{-a})}$. Then only $E_{2;c_1,c_1'}$ can contain the configurations of type (2-a) and nontrivially contribute to the integral.

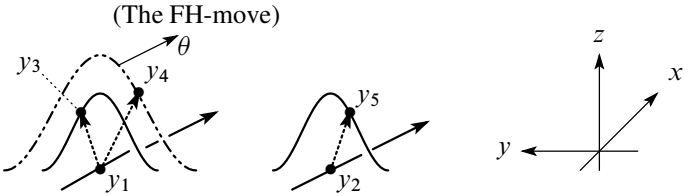

Figure 18. Proof of Proposition 4.6.

The proof of this case goes very similarly to the above ones; we just need to replace

- (4-25) and (4-26) respectively with

$$\begin{aligned} y_1 &= (x_1, 0, 0), \\ y_2 &= (x_2, 0, 0), \\ y_3 &= (0, -\epsilon_2 x_3, b(\epsilon_2 x_3)), \\ y_4 &= (\theta, -\epsilon_1 x_4, 2b(\epsilon_1 x_4/2)), \\ y_5 &= (0, \epsilon_3 x_5, b(\epsilon_3 x_5)), \end{aligned} \tag{4-37}$$

$$\varphi(\theta, x_1, \dots, x_5) := \left(\frac{y_3 - y_1}{|y_3 - y_1|}, \frac{y_5 - y_2}{|y_5 - y_2|}, \frac{y_4 - y_1}{|y_4 - y_1|} \right), \tag{4-38}$$

- (4-28) with

$$\Phi(\theta, x_1, \dots, x_5) := ((x_1, \epsilon_2 x_3), (x_1 - \theta, \epsilon_1 x_4), (x_2, \epsilon_3 x_5)). \tag{4-39}$$

Then Φ is a linear diffeomorphism with the determinant $-\epsilon_1\epsilon_2\epsilon_3$, and because we meet the situation (2-a) twice in the FH-cycle, the left hand side of (4-36) in this case is equal to

$$-2(\epsilon_1\epsilon_2\epsilon_3)^2 \left(\int_{\mathbb{R}^2} \psi_1^* \,\mathrm{vol} \right)^2 \int_{\mathbb{R}^2} \psi_2^* \,\mathrm{vol} = -\tfrac{1}{4}. \tag{4-40}$$

Consider the second case that c_1, c_2, c_3 respect the Gauss diagram $G_{(2\text{-b})}$. The proof of this case goes very similarly to that of the case (1-b) in Proposition 4.5; we just need to replace

- (4-25) and (4-26) respectively with

$$\begin{aligned} y_1 &= (x_1, 0, 0),\\ y_2 &= (x_2, 0, 0),\\ y_3 &= (\theta, -\epsilon_1 x_3, 2b(\epsilon_1 x_3/2)),\\ y_4 &= (0, -\epsilon_2 x_4, b(\epsilon_2 x_4)),\\ y_5 &= (0, \epsilon_3 x_5, b(\epsilon_3 x_5)), \end{aligned} \tag{4-41}$$

$$\varphi(\theta, x_1, \dots, x_5) := \left(\frac{y_4 - y_1}{|y_4 - y_1|}, \frac{y_5 - y_2}{|y_5 - y_2|}, \frac{y_3 - y_1}{|y_3 - y_1|} \right), \tag{4-42}$$

- (4-28) with

$$\Phi(\theta, x_1, \dots, x_5) := ((x_1 - \theta, \epsilon_2 x_3), (x_1, \epsilon_1 x_4), (x_2, \epsilon_3 x_5)). \tag{4-43}$$

Then Φ is a linear diffeomorphism with the determinant $\epsilon_1\epsilon_2\epsilon_3$, and because we meet the situation (2-b) six times in the FH-cycle, the left hand side of (4-36) in this case is equal to

$$6(\epsilon_1\epsilon_2\epsilon_3)^2 \left(\int_{\mathbb{R}^2} \psi_1^* \,\mathrm{vol} \right)^2 \int_{\mathbb{R}^2} \psi_2^* \,\mathrm{vol} = \tfrac{3}{4}. \tag{4-44}$$

□

Proof of Theorem 4.1. Let c_1, c_2 and c_3 respect one of the Gauss diagrams in Type I cycle (Figure 7). Then by (4-14) and Propositions 4.5, 4.6 we have

$$\begin{aligned} D^3 v(\tilde{f}) &= \sum_{k=1,2} a_k \sum_{c\in\{c_1,c_2,c_3\}} \sum_{\epsilon_1,\epsilon_2,\epsilon_3\in\{+1,-1\}} \epsilon_1\epsilon_2\epsilon_3 \int_{E_{k;c,c'}} \overline{p\circ FH_{\tilde{f}_{\epsilon_1,\epsilon_2,\epsilon_3}}}^{\,*} \omega_{X_k}\\ &= (-2)\cdot \sum_{\epsilon_1,\epsilon_2,\epsilon_3\in\{+1,-1\}} \tfrac{1}{8} + 1\cdot 0\\ &= -2\cdot\tfrac{1}{8}\cdot 8 = -2. \end{aligned} \tag{4-45}$$

Next suppose that c_1, c_2 and c_3 respect one of the Gauss diagrams in Type II cycle (Figure 7). Then by (4-14) and Propositions 4.5 and 4.6,

$$\begin{aligned} D^3 v(\tilde{f}) &= \sum_{k=1,2} a_k \sum_{c\in\{c_1,c_2,c_3\}} \sum_{\epsilon_1,\epsilon_2,\epsilon_3\in\{+1,-1\}} \epsilon_1\epsilon_2\epsilon_3 \int_{E_{k;c,c'}} \overline{p\circ FH_{\tilde{f}_{\epsilon_1,\epsilon_2,\epsilon_3}}}^{\,*} \omega_{X_k}\\ &= (-2)\cdot \sum_{\epsilon_1,\epsilon_2,\epsilon_3\in\{+1,-1\}} \left(-\tfrac{1}{4}\right) + 1\cdot \sum_{\epsilon_1,\epsilon_2,\epsilon_3\in\{+1,-1\}} \left(-\tfrac{1}{4}\right)\\ &= 2. \end{aligned} \tag{4-46}$$

Lastly suppose that c_1, c_2 and c_3 respect one of the Gauss diagrams in Type III cycle (Figure 7). Then

$$\begin{aligned}(4\text{-}47)\quad D^3v(\tilde{f}) &= \sum_{k=1,2} a_k \sum_{c\in\{c_1,c_2,c_3\}} \sum_{\epsilon_1,\epsilon_2,\epsilon_3\in\{+1,-1\}} \epsilon_1\epsilon_2\epsilon_3 \int_{E_{k;c,c'}} \overline{p\circ FH_{\tilde{f}_{\epsilon_1,\epsilon_2,\epsilon_3}}}^{*}\omega_{X_k} \\ &= (-2)\cdot 0 + 1\cdot \sum_{\epsilon_1,\epsilon_2,\epsilon_3\in\{+1,-1\}} \frac{3}{4} \\ &= 6.\end{aligned}$$

If c_1, c_2 and c_3 respect no Gauss diagram in three cycles, then $D^3v(\tilde{f}) = 0$. □

4C. ***An explicit description of v.*** It is known (see [12, page 215] for example) that the space of the Vassiliev invariants for framed knots of order less than or equal to three are multiplicatively generated by the framing number lk, the Casson invariant v_2 and the order three invariant v_3 (characterized by the conditions in Theorem 1.2). Thus all the Vassiliev invariants of order less than or equal to three are linear combinations of

$$(4\text{-}48)\qquad \mathrm{lk},\quad v_2,\quad \mathrm{lk}^2,\quad v_3,\quad \mathrm{lk}\cdot v_2,\quad \mathrm{lk}^3\,.$$

Lemma 4.7. *Our invariant v is of the form $v = av_3 + b\,\mathrm{lk}\cdot v_2 + cv_2$ for some constants $a, b, c \in \mathbb{R}$.*

Proof. The value of v on the trivial long knot $f_0(x) = (x, 0, 0)$ together with a framing number $w \in \mathbb{Z}$ is a linear combination of w, w^2 and w^3 because $v_2(f_0) = v_3(f_0) = 0$. But by the definition $p_*H_{(f_0,w)}$ is a constant loop of $\mathcal{K}$ for any $w \in \mathbb{Z}$. Thus $v(f_0, w) = 0$ for any $w \in \mathbb{Z}$, and the coefficients of lk, lk^2 and lk^3 must be zero. □

Below we compute the constants a, b, c in Lemma 4.7. We denote by 3_1^+ and 3_1^- respectively the right-handed and the left-handed trefoil knots, by 4_1 the figure eight knot. By the formulas for v_2 and v_3 in [15, Theorems 1 and 2] we have

$$(4\text{-}49)\qquad v_2(3_1^+) = v_2(3_1^-) = 1,\quad v_2(4_1) = -1,\quad v_3(4_1) = 0.$$

Proposition 4.8. *We have $a = 6$, $b = -1$.*

Proof. Consider the "standard" diagram of 3_1^+ in Figure 2 and write it as $f = f_{+,+,+}$. This can be seen as a framed long knot with framing number $+3$. The diagram $f_{-,-,-}$ is 3_1^- with framing number -3 and all the other $f_{\epsilon_1,\epsilon_2,\epsilon_3}$ are trivial. The Gauss diagram in Figure 2 appears in the Type III cycle in Figure 9 and $D^3v(f) = 6$

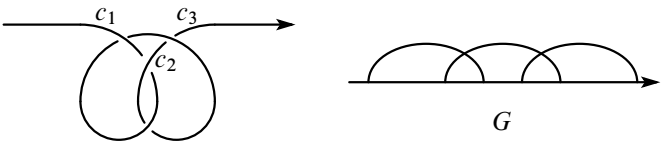

Figure 19. A diagram of $g = 4_1$ and the Gauss diagram that c_1, c_2, c_3 respect.

by Theorem 4.1. Thus we have

$$\begin{aligned}(4\text{-}50)\qquad 6 &= D^3v(f)\\ &= (av_3(3_1^+) + b\cdot 3 + cv_2(3_1^+)) - (av_3(3_1^-) + b\cdot(-3) + cv_2(3_1^-))\\ &= 2a + 6b,\end{aligned}$$

here the last equality holds by (4-49).

Next consider the diagram of 4_1 in Figure 19.

We write it as $g = g_{+,-,+}$, focusing on c_1, c_2, c_3. This can be seen as a framed long knot with framing number 0. Then $g_{-,-,-}$ is the 3_1^- with framing number -4 and all the other $g_{\epsilon_1,\epsilon_2,\epsilon_3}$ are trivial. The Gauss diagram G in Figure 19 appears in the Type II cycle in Figure 8 and $D^3v(g) = 2$ by Theorem 4.1. Thus we have

$$\begin{aligned}(4\text{-}51)\qquad 2 &= D^3v(g)\\ &= -(av_3(4_1) + b\cdot 0 + cv_2(4_1)) - (av_3(3_1^-) + b\cdot(-4) + cv_2(3_1^-))\\ &= a + 4b,\end{aligned}$$

here the last equality holds again by (4-49). Therefore $a = 6$, $b = -1$ by (4-50) and (4-51). □

Corollary 4.9 [17, Theorem 3.1]. *$\int_{G_f} I(X) = v_2(f)$ for any $f \in \mathcal{K}$.*

Proof. It is not hard to see that $p_*FH_{(f,w+1)} = p_*FH_{(f,w)} - G_f$ for any $f \in \mathcal{K}$ and $w \in \mathbb{Z}$. Thus we have

$$\begin{aligned}(4\text{-}52)\qquad v(f, w+1) &= \int_{p_*FH_{(f,w+1)}} I(X)\\ &= \int_{p_*FH_{(f,w)}} I(X) - \int_{G_f} I(X)\\ &= v(f, w) - \int_{G_f} I(X).\end{aligned}$$

Since $v = 6v_3 - \mathrm{lk}\cdot v_2 + cv_2$,

$$(4\text{-}53)\quad 6v_3(f) - (w+1)v_2(f) + cv_2(f) = 6v_3(f) - wv_2(f) + cv_2 - \int_{G_f} I(X),$$

implying $\int_{G_f} I(X) = v_2(f)$. □

Proposition 4.10. *We have* $c = 0$.

Proof. Let $\tilde{f}$ be the knot 3_1^+ with the blackboard framing from the planar projection in Figure 2. Its framing number is $+3$, and as explained in [11], the FH-cycle $p_*FH_{\tilde{f}}$ is homologous to 3 times the Gramain cycle G_f (see Remark 3.4), where $f = p(\tilde{f}) \in \mathcal{K}$. This is because, as we can see in the figure in [11, page 4], the FH-move on each crossing of $\tilde{f}$ is the rotation around the long axis by degree π, and in the FH-cycle we perform the FH-moves six times. Thus

$$6v_3(3_1^+) - 3v_2(3_1^+) + cv_2(3_1^+) = v(\tilde{f}) = \int_{p_*FH_{\tilde{f}}} I(X) = 3\int_{G_f} I(X). \tag{4-54}$$

Corollary 4.9 allows us to rewrite (4-54) as

$$6 \cdot 1 - 3 \cdot 1 + c \cdot 1 = 3 \cdot 1, \tag{4-55}$$

and we have $c = 0$. □

This completes the proof of the formula $I(X) = 6v_3 - \mathrm{lk} \cdot v_2$ in Theorem 1.2.

Remark 4.11. In fact the proof of [17, Theorem 3.1] seems to contain an error. In [17, page 414] the second named author of the present paper claimed that "the zero-cycle e is given by $(\iota, 1)$", but e is indeed given by $(\iota, 2)$. Thus [17, Lemma 3.4] has to be corrected as "$D^2V(f) = \frac{1}{2}$" and consequently the evaluation of $I(X)$ over G_f should be $v_2(f)/2$, inconsistent with Corollary 4.9. Probably the proof of Corollary 4.9 is correct and this inconsistency comes from a missing factor of 2 in [16, Lemma 4.5], a special case of which ($n = 3$) is [17, Lemma 3.4].

Remark 4.12. An anonymous referee kindly suggested that the formula (1-1) in Theorem 1.2 can recover a result of Alvarez and Labastida [2]

$$v_3(T_{m,n}) = \frac{mn}{6} v_2(T_{m,n}) \tag{4-56}$$

for the (m, n)-torus (long) knot $T_{m,n}$.

The proof goes as follows. Let $\tilde{f}$ be a framed long knot whose underlying long knot is $f = p(\tilde{f}) = T_{m,n}$ and framing number $\mathrm{lk}(\tilde{f}) = w$. Then the formulas (1-1) and [17, Theorem 3.1] together with the fact that G_f generates $\pi_1(\mathcal{K}_f) \cong \mathbb{Z}$ if $f = T_{m,n}$ imply that $p_*FH_{\tilde{f}} = k(w)G_f$ for some $k(w) \in \mathbb{Z}$ and

$$6v_3(f) - w \cdot v_2(f) = \int_{p_*FH_{\tilde{f}}} I(X) = \int_{k(w)G_f} I(X) = k(w)v_2(f). \tag{4-57}$$

We can see that $k(mn) = 0$, proving the formula (4-56). To see this, we regard the space of framed long knots as that of framed embeddings $S^1 \hookrightarrow S^3$ that preserve

the basepoints and have a prescribed framing at the basepoint, as explained in Section 2A. Then we have a homeomorphism

$$\widetilde{\mathrm{Emb}}(S^1, S^3) \approx \widetilde{\mathcal{K}} \times \mathrm{SO}(4), \quad \tilde{f} \mapsto (A^{-1} \cdot \tilde{f}, A(0)) \tag{4-58}$$

where $\widetilde{\mathrm{Emb}}(S^1, S^3)$ is the space of framed embeddings $S^1 \hookrightarrow S^3$ (without any basepoint conditions), $A\colon S^1 \to \mathrm{SO}(4)$ is the map given in Section 2A and $0 \in S^1 = [0, 1]/(0 \simeq 1)$ is the basepoint of S^1. This homeomorphism induces

$$\widetilde{\mathcal{K}} \approx \widetilde{\mathrm{Emb}}(S^1, S^3)/\mathrm{SO}(4) \tag{4-59}$$

and the Fox–Hatcher S^1-action on $\widetilde{\mathcal{K}}$ is interpreted as the reparametrization on the right hand side.

If $f = T_{m,n}$ is placed on the torus $\{(z, w) \in S^3 \mid |z| = |w| = 1/\sqrt{2}\}$ in the standard way, and if f is given the framing mn, then the reparametrization of $\tilde{f} = (f, mn) \in \widetilde{\mathrm{Emb}}(S^1, S^3)$ by $t \in S^1$ can be described as the multiplication of

$$r_{m,n}(t) = \begin{pmatrix} e^{2\pi\sqrt{-1}\,mt} & 0 \\ 0 & e^{2\pi\sqrt{-1}\,nt} \end{pmatrix} \in \mathrm{SO}(4). \tag{4-60}$$

In other words $FH_{(T_{m,n},mn)}$ is trivial on $\widetilde{\mathrm{Emb}}(S^1, S^3)/\mathrm{SO}(4)$ and thus on $\widetilde{\mathcal{K}}$. Therefore we have $k(mn) = 0$.

Acknowledgments

The authors are deeply grateful to Arnaud Mortier for their invaluable comments and discussions. They also express their appreciation to Thomas Fiedler for sharing the information about his 1-cocycles in his book. The comments of anonymous referees are of great worth for the authors. Part of this work is based on the master thesis of the first named author and she expresses her gratitude to her colleagues Yukiho Tomeba and Yuiko Yamanouchi for their support.

References

[1] D. Altschuler and L. Freidel, "Vassiliev knot invariants and Chern–Simons perturbation theory to all orders", *Comm. Math. Phys.* **187**:2 (1997), 261–287. MR Zbl

[2] M. Alvarez and J. M. F. Labastida, "Vassiliev invariants for torus knots", *J. Knot Theory Ramifications* **5**:6 (1996), 779–803. MR Zbl

[3] S. Axelrod and I. M. Singer, "Chern–Simons perturbation theory, II", *J. Differential Geom.* **39**:1 (1994), 173–213. MR Zbl

[4] R. Bott and C. Taubes, "On the self-linking of knots", *J. Math. Phys.* **35**:10 (1994), 5247–5287. MR Zbl

[5] R. Budney, "Little cubes and long knots", *Topology* **46**:1 (2007), 1–27. MR Zbl

[6] A. S. Cattaneo, P. Cotta-Ramusino, and R. Longoni, "Configuration spaces and Vassiliev classes in any dimension", *Algebr. Geom. Topol.* **2** (2002), 949–1000. MR Zbl

[7] T. Fiedler, *Polynomial one-cocycles for knots and closed braids*, Series on Knots and Everything **64**, World Scientific, Hackensack, NJ, 2020. MR Zbl

[8] T. Fiedler, "Polynomial invariants which can distinguish the orientations of knots", preprint, 2022. arXiv 2211.10734

[9] R. H. Fox, "Rolling", *Bull. Amer. Math. Soc.* **72** (1966), 162–164. MR Zbl

[10] B. Gros and B. Zhang, "A combinatorial one-cocycle in a moduli space of knots from the Vassiliev invariant of order 3", preprint, 2022. arXiv 2212.03778

[11] A. Hatcher, "Topological moduli space of knots", unfinished draft, 2022, available at https://pi.math.cornell.edu/~hatcher/Papers/knotspaces.pdf.

[12] D. M. Jackson and I. Moffatt, *An introduction to quantum and Vassiliev knot invariants*, Springer, 2019. MR Zbl

[13] T. Kohno, "Vassiliev invariants and de Rham complex on the space of knots", pp. 123–138 in *Symplectic geometry and quantization* (Sanda and Yokohama, 1993), edited by Y. Maeda et al., Contemp. Math. **179**, Amer. Math. Soc., Providence, RI, 1994. MR Zbl

[14] A. Mortier, "Combinatorial cohomology of the space of long knots", *Algebr. Geom. Topol.* **15**:6 (2015), 3435–3465. MR Zbl

[15] M. Polyak and O. Viro, "Gauss diagram formulas for Vassiliev invariants", *Internat. Math. Res. Notices* 11 (1994), 445–453. MR Zbl

[16] K. Sakai, "Nontrivalent graph cocycle and cohomology of the long knot space", *Algebr. Geom. Topol.* **8**:3 (2008), 1499–1522. MR Zbl

[17] K. Sakai, "An integral expression of the first nontrivial one-cocycle of the space of long knots in $\mathbb{R}^3$", *Pacific J. Math.* **250**:2 (2011), 407–419. MR Zbl

[18] K. Sakai, "BV-structures on the homology of the framed long knot space", *J. Homotopy Relat. Struct.* **11**:3 (2016), 425–441. MR Zbl

[19] V. Turchin, "Computation of the first nontrivial 1-cocyle in the space of long knots", *Mat. Zametki* **80**:1 (2006), 105–114. MR

[20] I. Volić, "A survey of Bott–Taubes integration", *J. Knot Theory Ramifications* **16**:1 (2007), 1–42. MR Zbl

Received April 3, 2022. Revised February 28, 2023.

SAKI KANOU
FACULTY OF MATHEMATICS
SHINSHU UNIVERSITY
MATSUMOTO
JAPAN
20ss104f@gmail.com

KEIICHI SAKAI
FACULTY OF MATHEMATICS
SHINSHU UNIVERSITY
MATSUMOTO
JAPAN
sakaik@shinshu-u.ac.jp

PACIFIC JOURNAL OF MATHEMATICS

Founded in 1951 by E. F. Beckenbach (1906–1982) and F. Wolf (1904–1989)

msp.org/pjm

See inside back cover or msp.org/pjm for submission instructions.

The subscription price for 2023 is US $605/year for the electronic version, and $820/year for print and electronic.
Subscriptions, requests for back issues and changes of subscriber address should be sent to Pacific Journal of Mathematics, P.O. Box 4163, Berkeley, CA 94704-0163, U.S.A. The Pacific Journal of Mathematics is indexed by Mathematical Reviews, Zentralblatt MATH, PASCAL CNRS Index, Referativnyi Zhurnal, Current Mathematical Publications and Web of Knowledge (Science Citation Index).

The Pacific Journal of Mathematics (ISSN 1945-5844 electronic, 0030-8730 printed) at the University of California, c/o Department of Mathematics, 798 Evans Hall #3840, Berkeley, CA 94720-3840, is published twelve times a year. Periodical rate postage paid at Berkeley, CA 94704, and additional mailing offices. POSTMASTER: send address changes to Pacific Journal of Mathematics, P.O. Box 4163, Berkeley, CA 94704-0163.

PJM peer review and production are managed by EditFLOW® from Mathematical Sciences Publishers.

PUBLISHED BY

mathematical sciences publishers

nonprofit scientific publishing

http://msp.org/

PACIFIC JOURNAL OF MATHEMATICS

Volume 323 No. 2 April 2023